Supporting Information for:

Solvent-Free Synthesis and Thin-Film Deposition of Cesium Copper Halides with Bright Blue Photoluminescence

Paz Sebastia-Luna, Javier Navarro-Alapont, Michele Sessolo, Francisco Palazon,* and Henk J. Bolink

Instituto de Ciencia Molecular, ICMol, Universidad de Valencia, C/ Catedrático J. Beltrán 2, 46980 Paterna, Spain

Table S 1. Lattice parameters derived from Le Bail fits of $CsCu_2X_3$ compounds (space group = Cmcm).

X	a (Å)	b (Å)	c (Å)	α (º)	β (º)	γ (º)	V (Å^3)
I	10.50438	13.11778	6.08282	90	90	90	838
$I_{75}Br_{25}$	10.47270	13.14974	6.06720	90	90	90	836
$I_{50}Br_{50}$	10.00890	12.91363	5.98059	90	90	90	773
$I_{25}Br_{75}$	9.78000	12.67451	5.91661	90	90	90	733
Br	9.87500	12.35396	5.81609	90	90	90	710
$Cl_{25}Br_{75}$	9.73313	12.29817	5.77289	90	90	90	691
$Cl_{50}Br_{50}$	9.58554	12.19961	5.71844	90	90	90	669
$Cl_{75}Br_{25}$	9.47997	12.09300	5.67565	90	90	90	651
Cl	9.50509	11.89780	5.59920	90	90	90	633

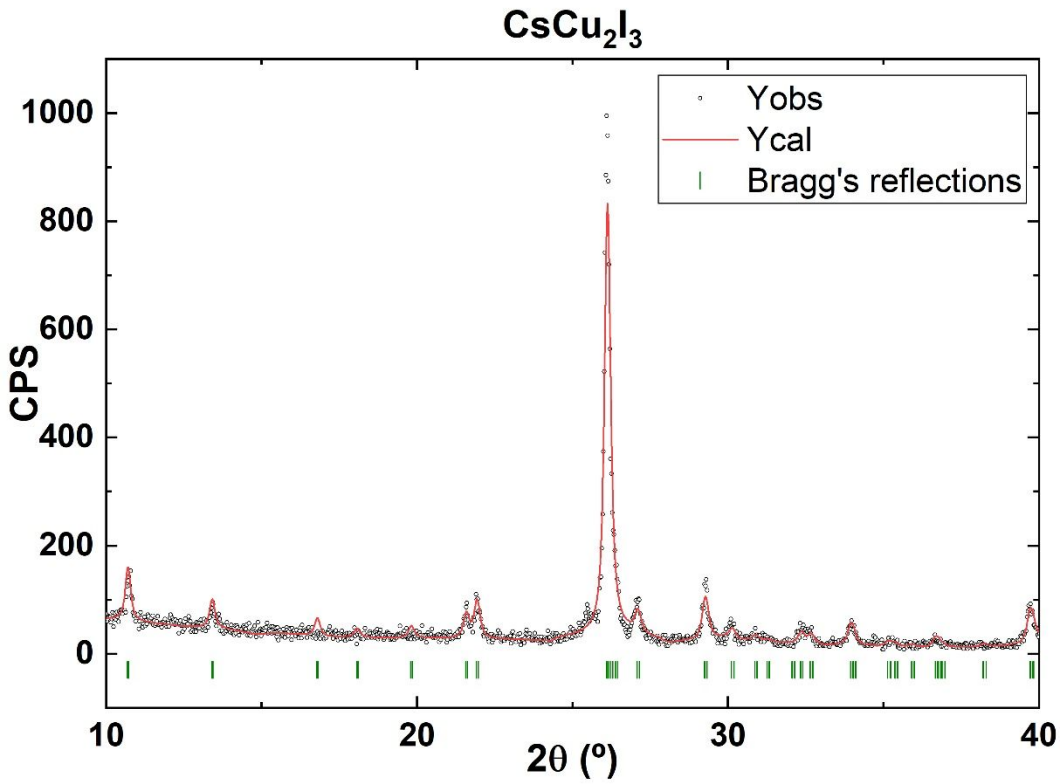

Figure S 1. Experimental (open circles) and fitted (red line) diffractograms. Caculated Bragg's reflections position in green. Compound given in title.

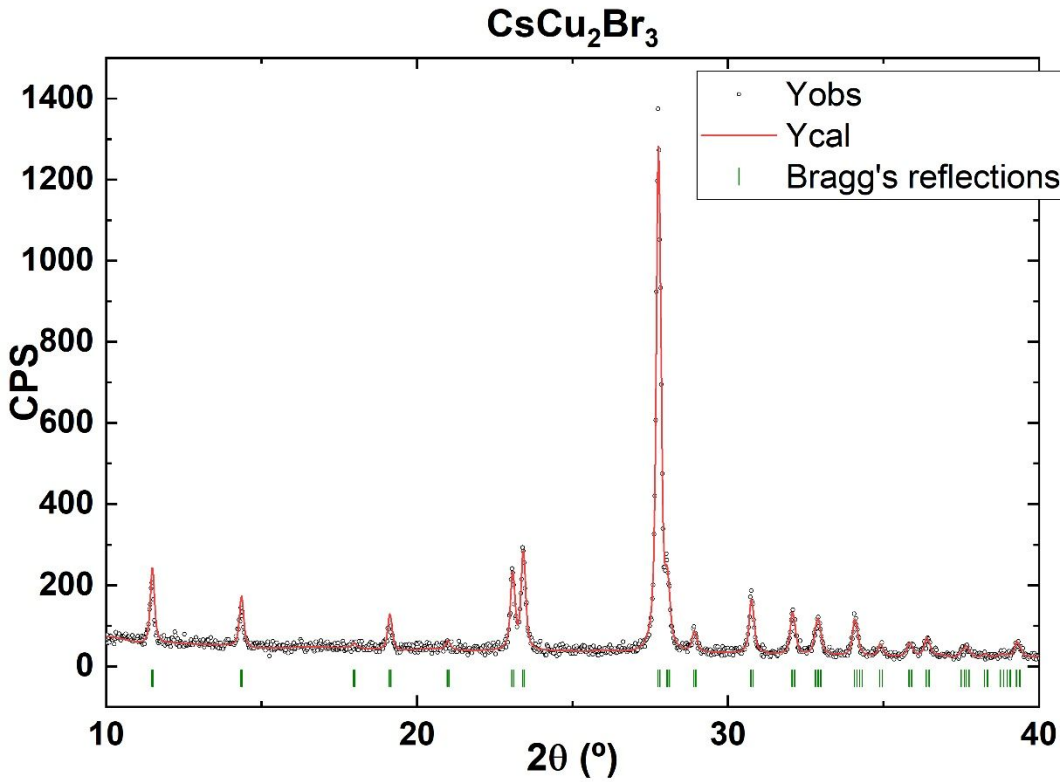

Figure S 2. Experimental (open circles) and fitted (red line) diffractograms. Caculated Bragg's reflections position in green. Compound given in title.

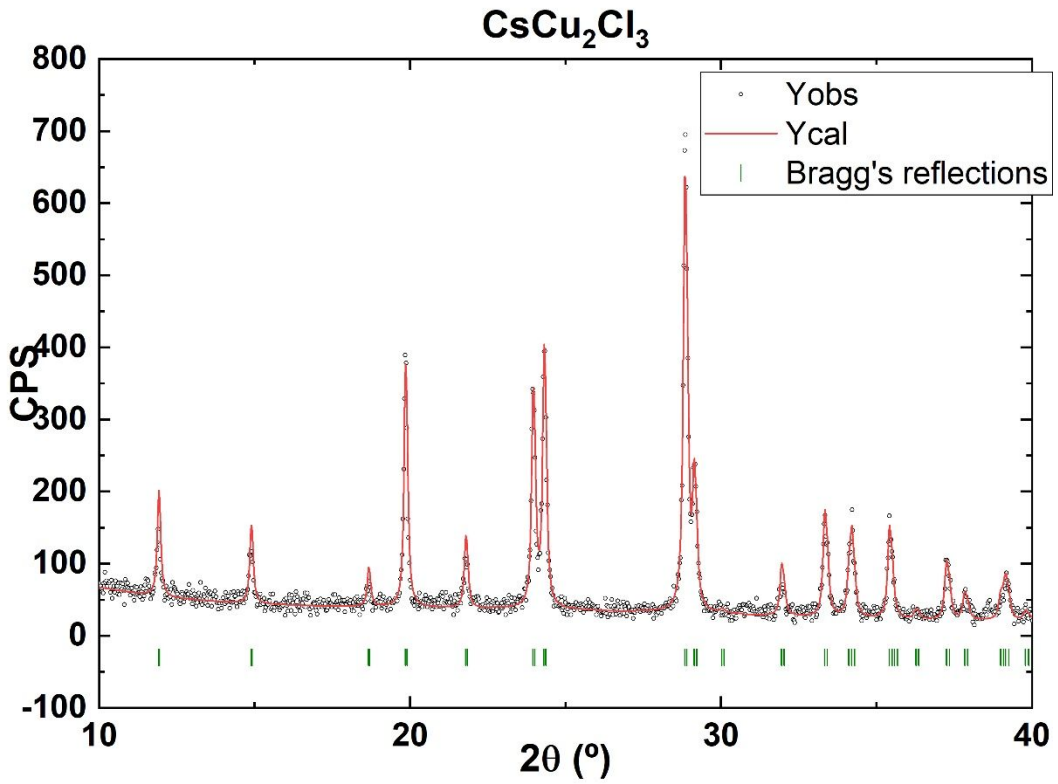

Figure S 3. Experimental (open circles) and fitted (red line) diffractograms. Caculated Bragg's reflections position in green. Compound given in title.

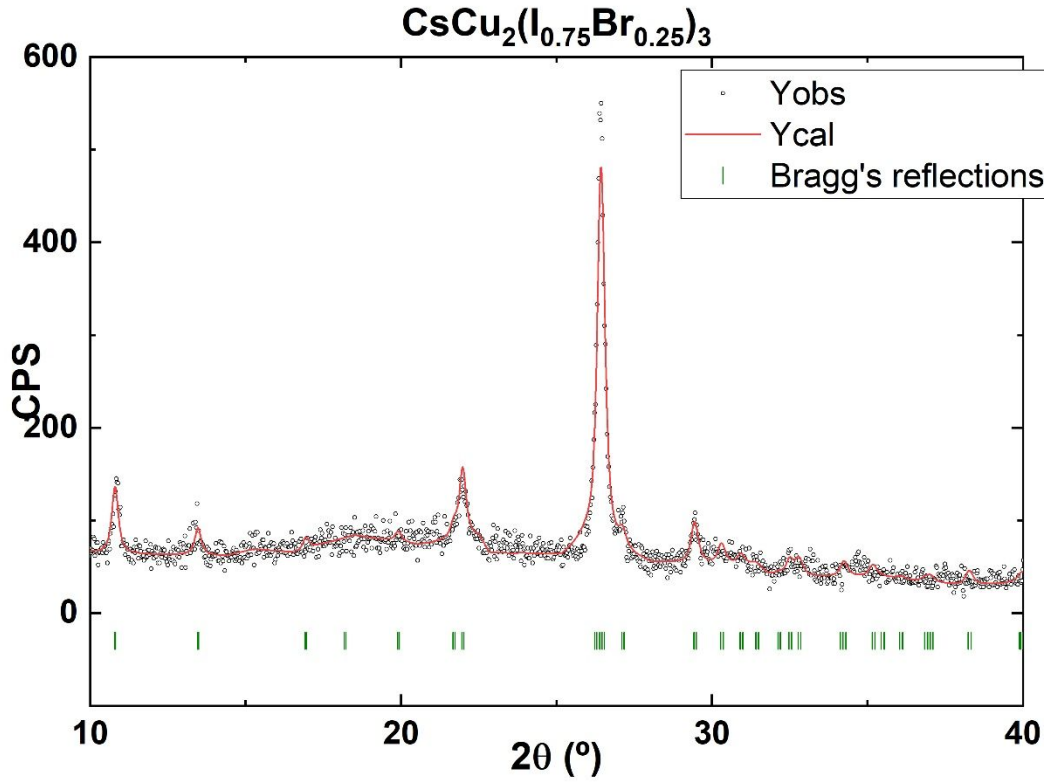

Figure S 4. Experimental (open circles) and fitted (red line) diffractograms. Caculated Bragg's reflections position in green. Compound given in title.

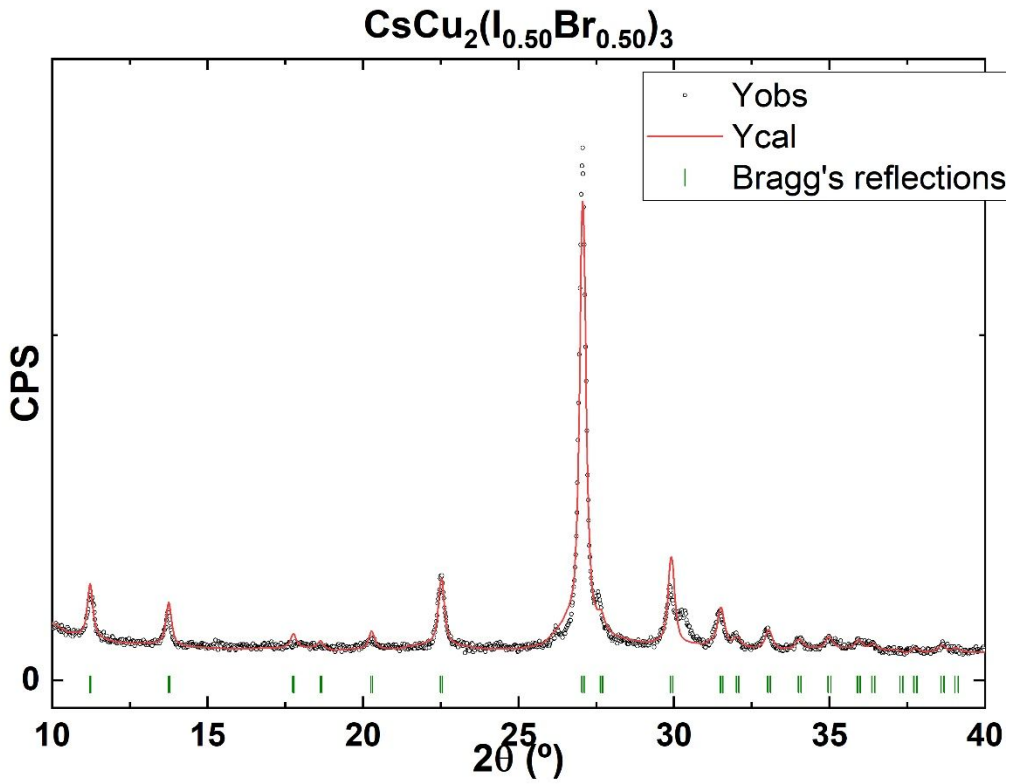

Figure S 5. Experimental (open circles) and fitted (red line) diffractograms. Caculated Bragg's reflections position in green. Compound given in title.

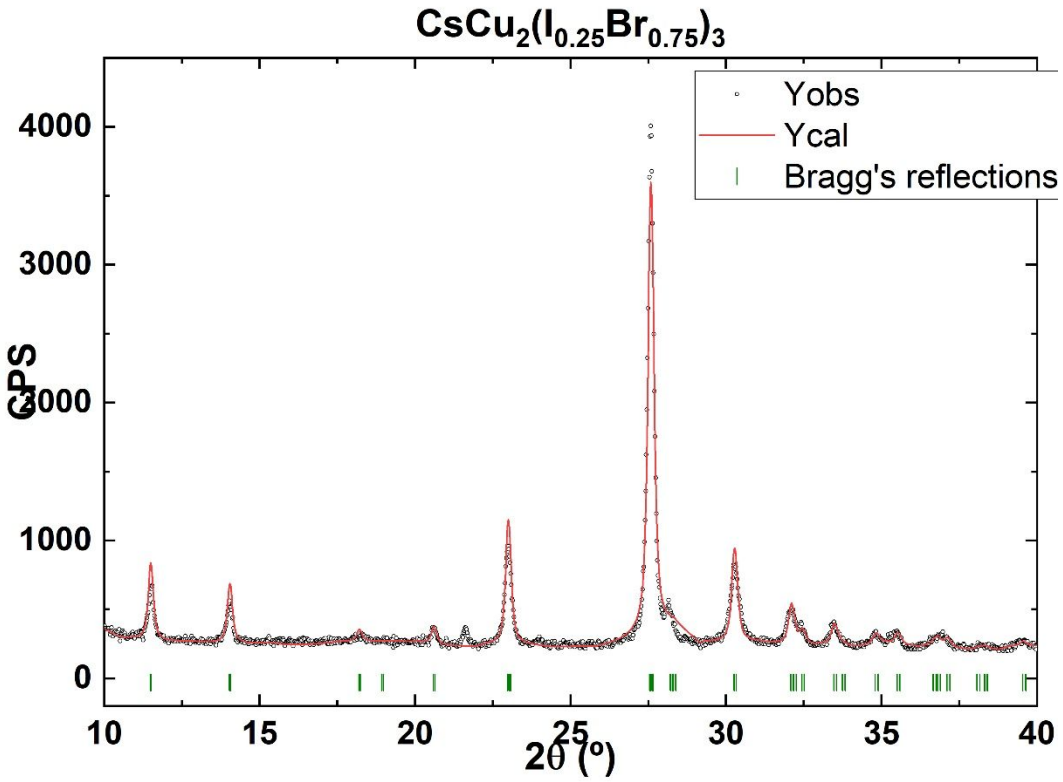

Figure S 6. Experimental (open circles) and fitted (red line) diffractograms. Caculated Bragg's reflections position in green. Compound given in title.

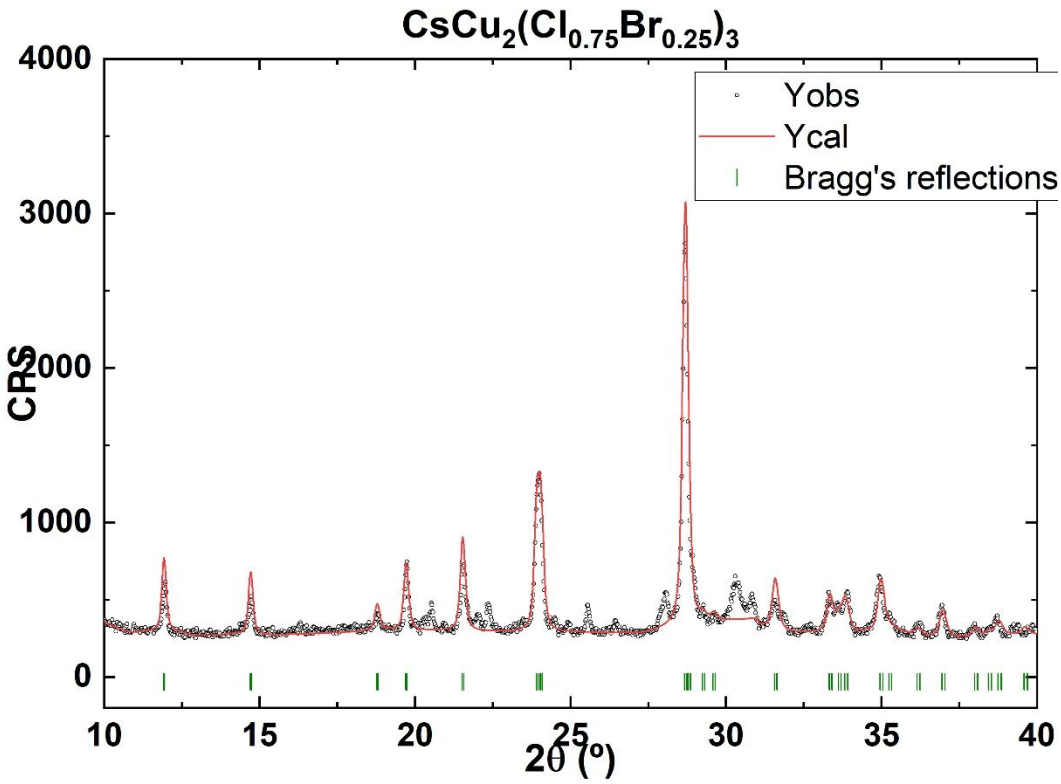

Figure S 7. Experimental (open circles) and fitted (red line) diffractograms. Caculated Bragg's reflections position in green. Compound given in title.

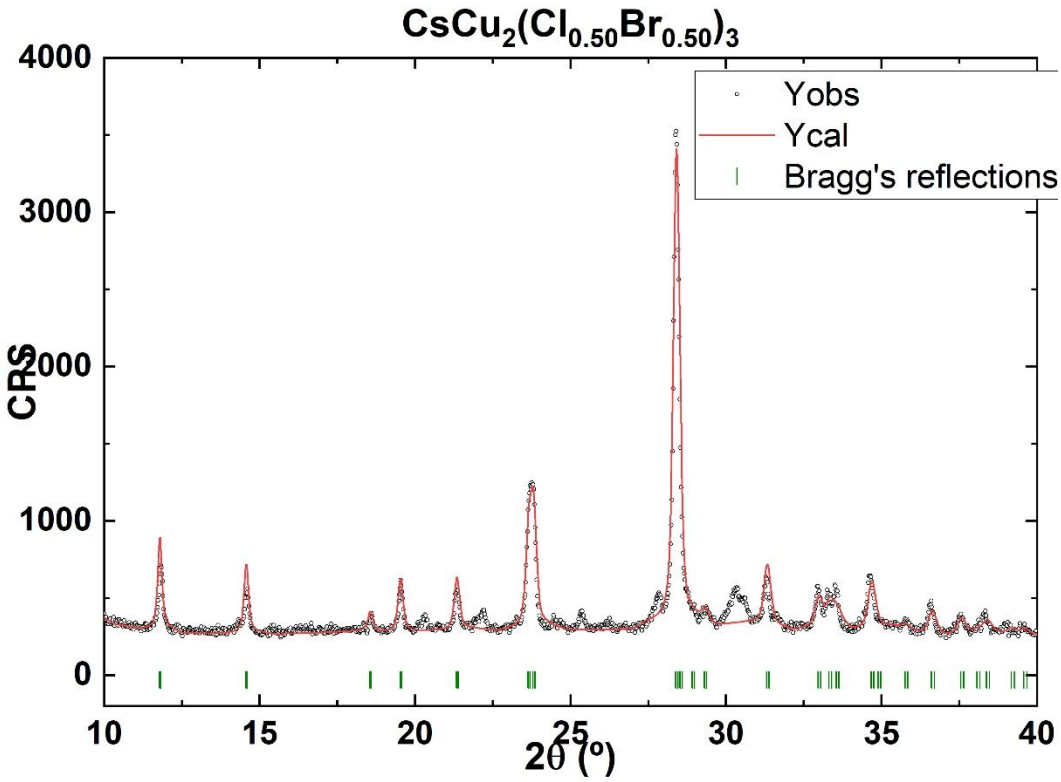

Figure S 8. Experimental (open circles) and fitted (red line) diffractograms. Caculated Bragg's reflections position in green. Compound given in title.

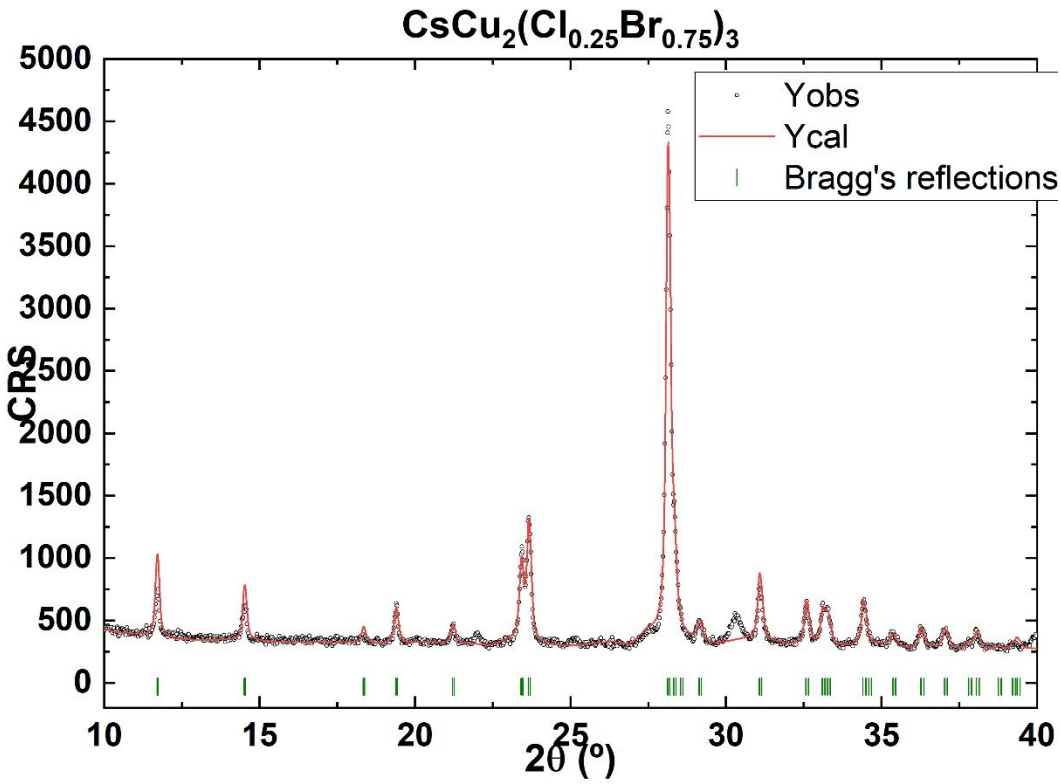

Figure S 9. Experimental (open circles) and fitted (red line) diffractograms. Caculated Bragg's reflections position in green. Compound given in title.

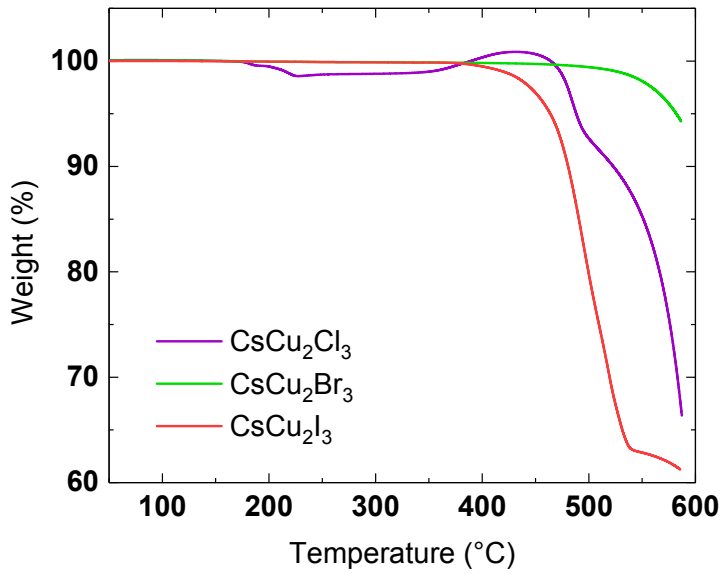

Figure S 10. Thermogravimetric analysis (TGA) of the pure-halide $CsCu_2X_3$ compounds.

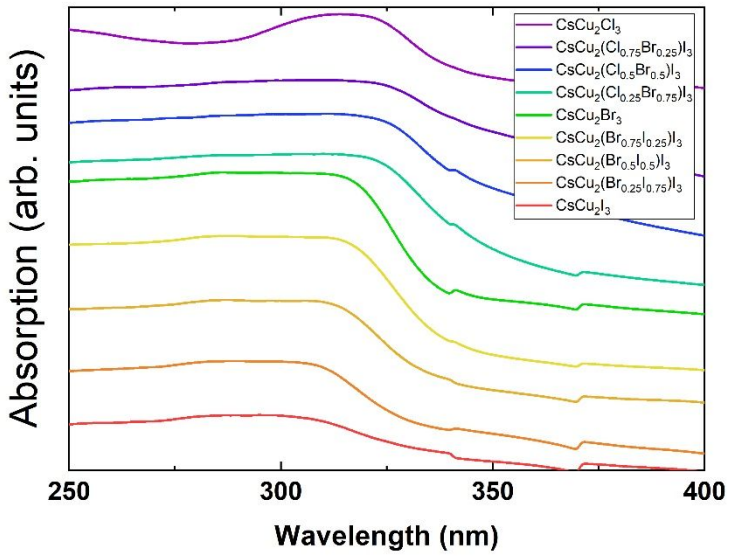

Figure S 11. Normalized absorbance spectra of powders of all CsCu2X3 compounds.

Table S 2. Lattice parameters derived from Le Bail fits of $Cs_3Cu_2X_5$ compounds (space group = Pnma for all compounds except for $Cs_3Cu_2X_5$ for which Cmcm is assumed).

X	a (Å)	b (Å)	c (Å)	α (º)	β (º)	γ (º)	V (Å^3)
I	10.16984	11.64503	14.36164	90	90	90	1701
$I_{75}Br_{25}$	9.61720	11.02493	13.66381	90	90	90	1634
$I_{50}Br_{50}$	9.81536	11.32985	14.00074	90	90	90	1557
$I_{25}Br_{75}$	9.70827	11.10062	13.70945	90	90	90	1477
Br	9.56618	10.92152	13.57964	90	90	90	1419
$Cl_{25}Br_{75}$	9.41863	10.79131	13.42943	90	90	90	1364
$Cl_{50}Br_{50}$	9.35090	10.68736	13.27232	90	90	90	1326
$Cl_{75}Br_{25}$	9.28622	10.59379	13.22188	90	90	90	1300
Cl	*15.42572*	*8.74765*	*8.67929*	*90*	*90*	*90*	*1171*

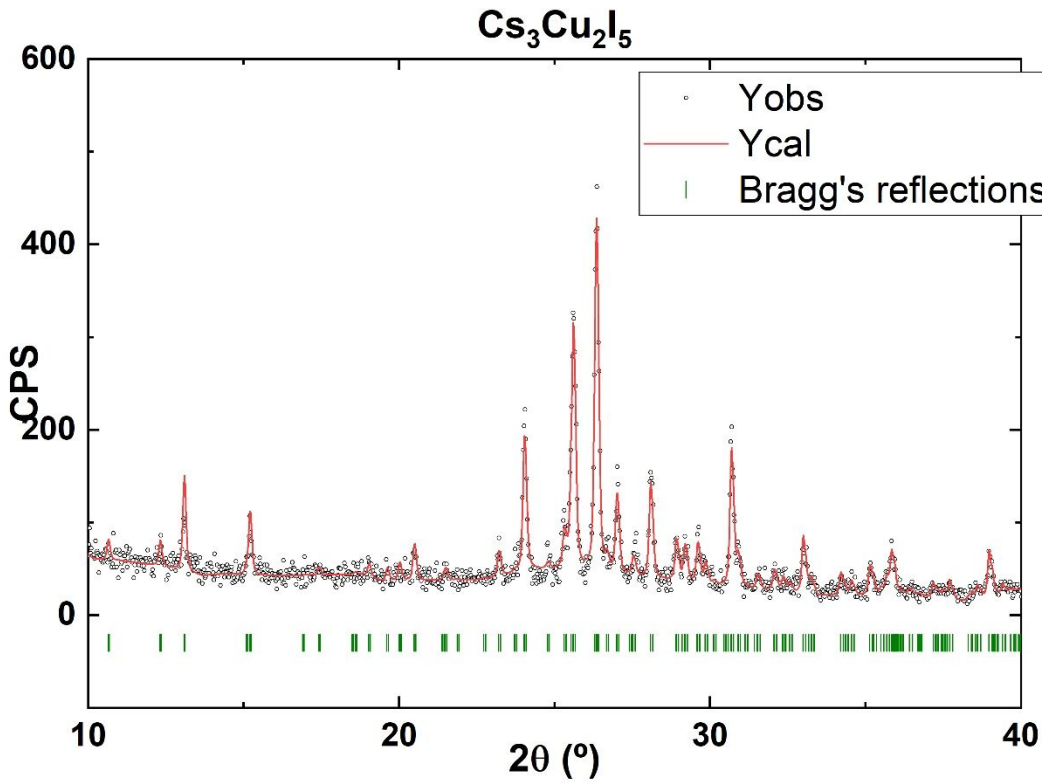

Figure S 12. Experimental (open circles) and fitted (red line) diffractograms. Caculated Bragg's reflections position in green. Compound given in title.

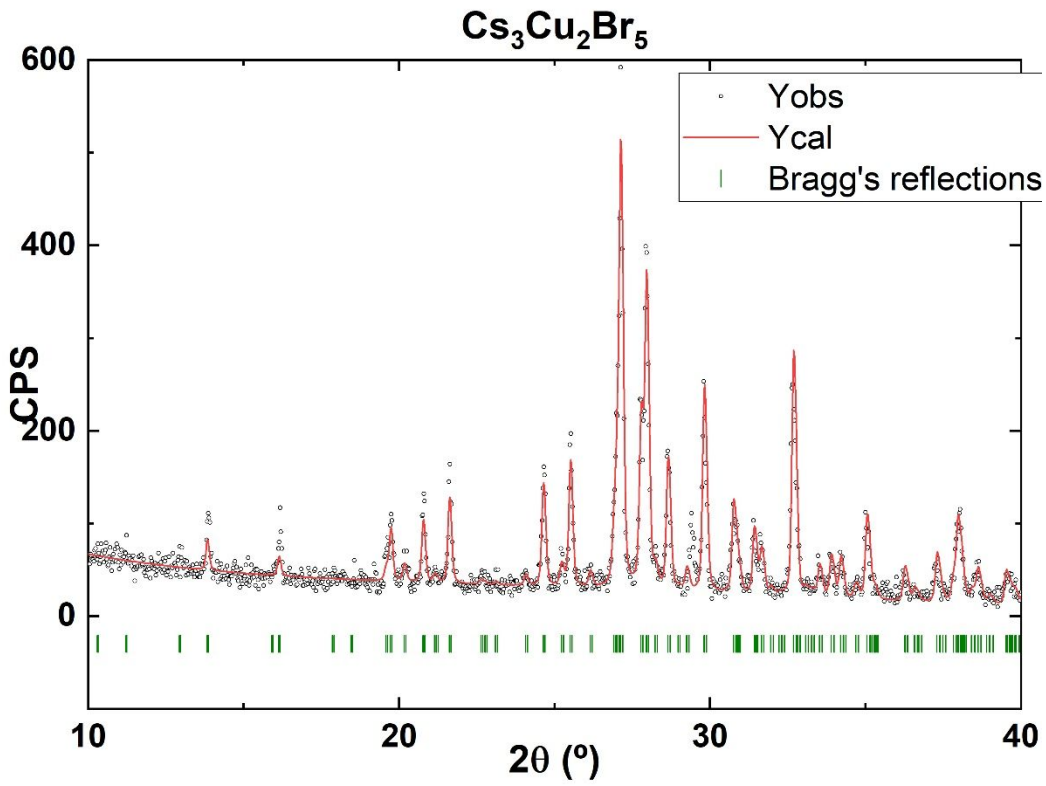

Figure S 13. Experimental (open circles) and fitted (red line) diffractograms. Caculated Bragg's reflections position in green. Compound given in title.

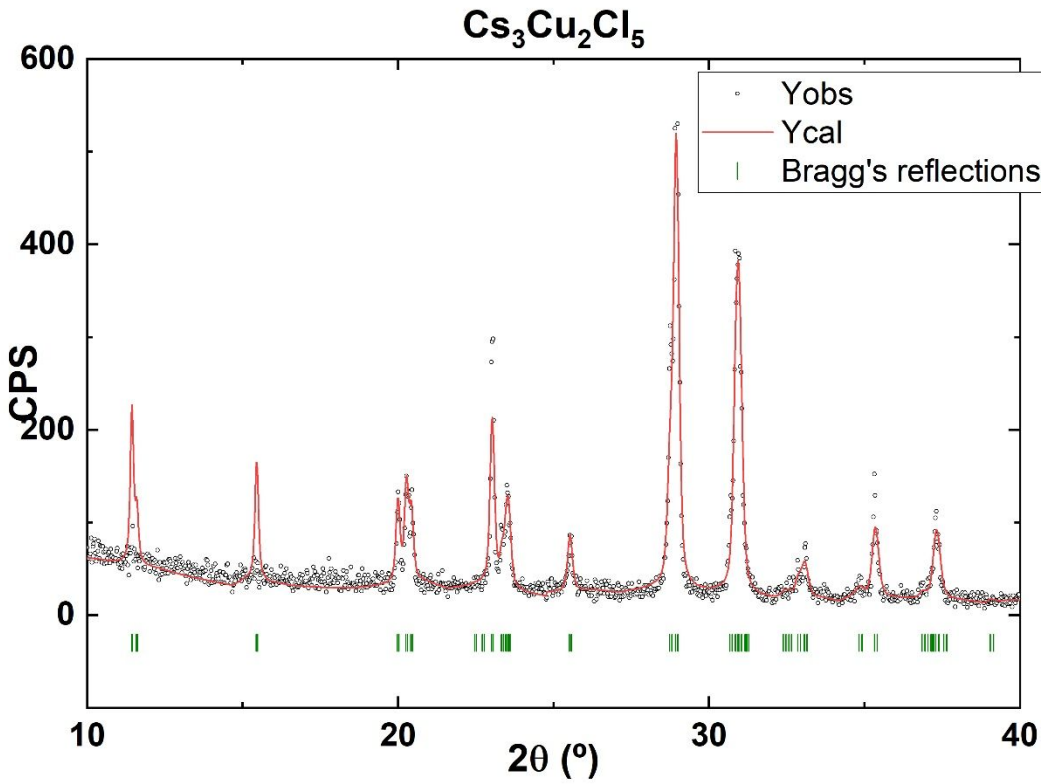

Figure S 14. Experimental (open circles) and fitted (red line) diffractograms. Caculated Bragg's reflections position in green. Compound given in title.

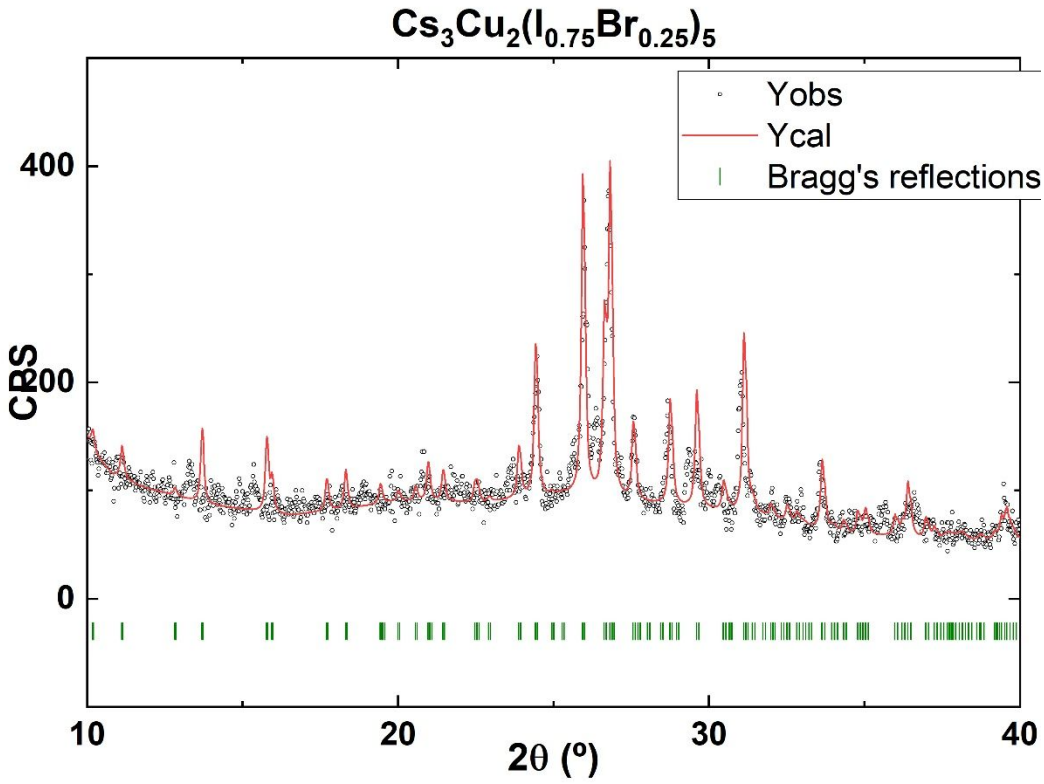

Figure S 15. Experimental (open circles) and fitted (red line) diffractograms. Caculated Bragg's reflections position in green. Compound given in title.

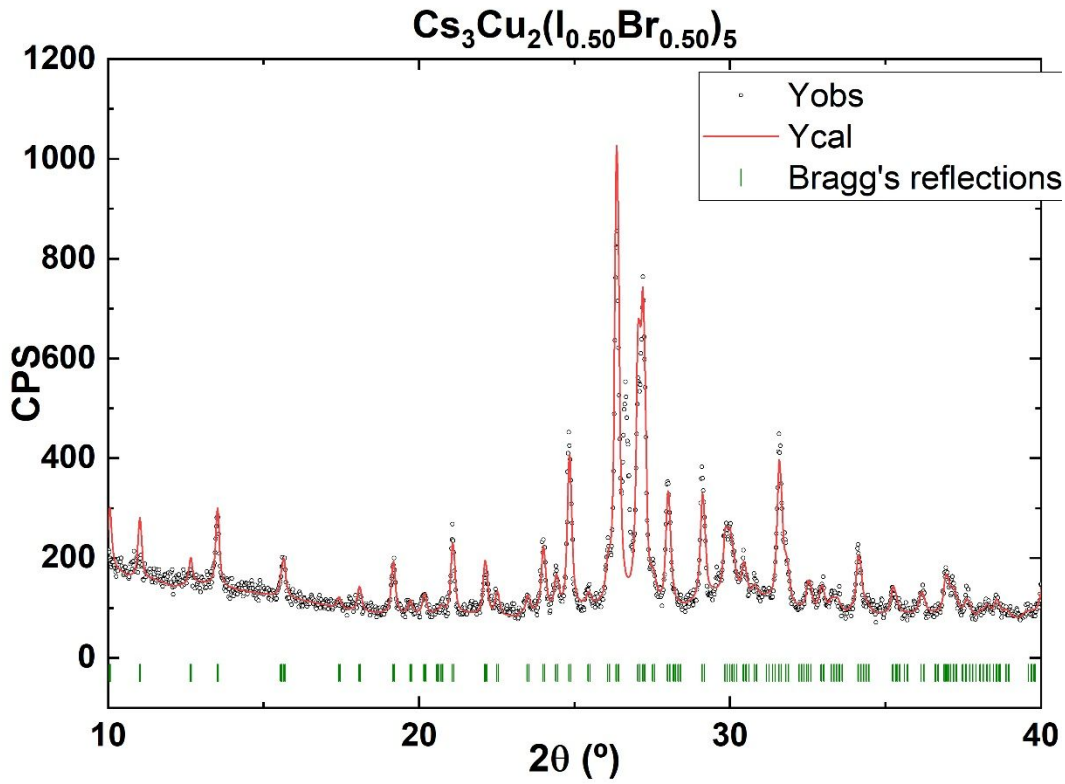

Figure S 16. Experimental (open circles) and fitted (red line) diffractograms. Caculated Bragg's reflections position in green. Compound given in title.

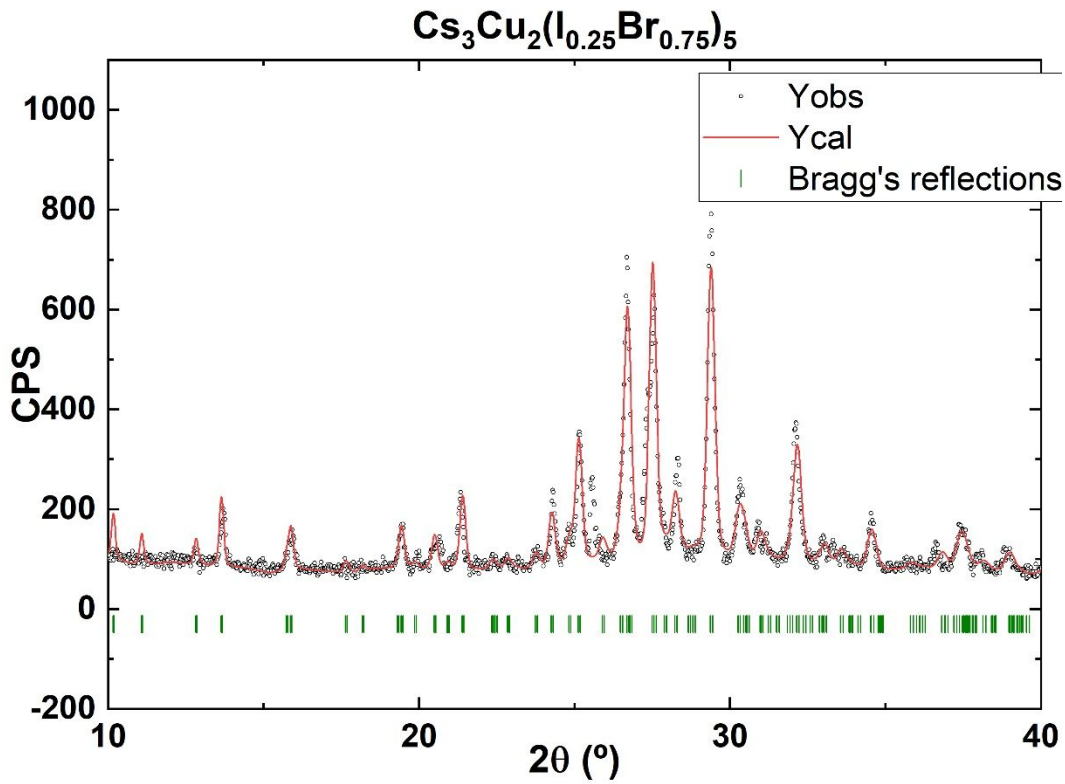

Figure S 17. Experimental (open circles) and fitted (red line) diffractograms. Caculated Bragg's reflections position in green. Compound given in title.

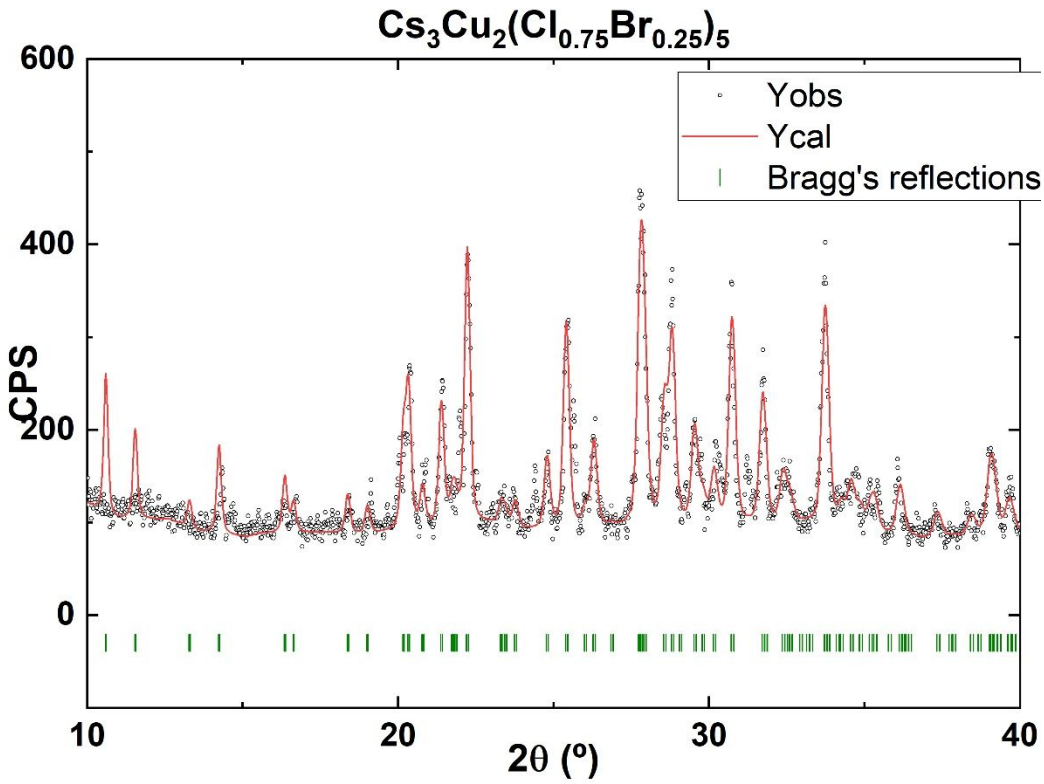

Figure S 18. Experimental (open circles) and fitted (red line) diffractograms. Caculated Bragg's reflections position in green. Compound given in title.

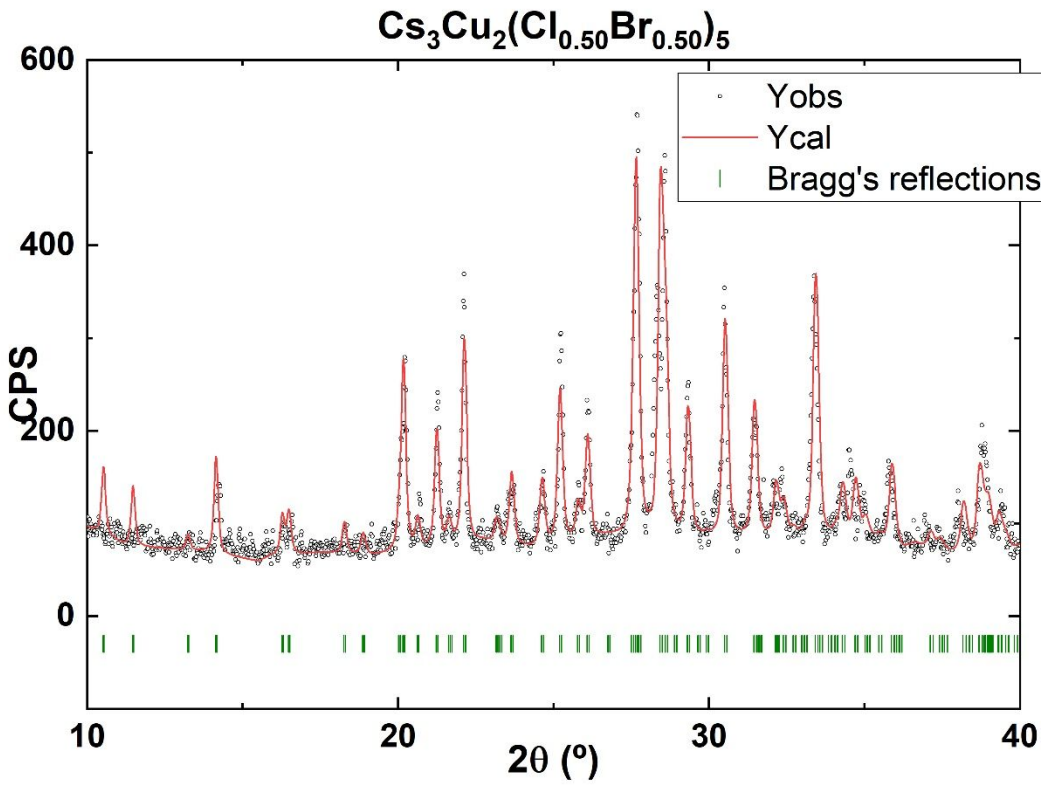

Figure S 19. Experimental (open circles) and fitted (red line) diffractograms. Caculated Bragg's reflections position in green. Compound given in title.

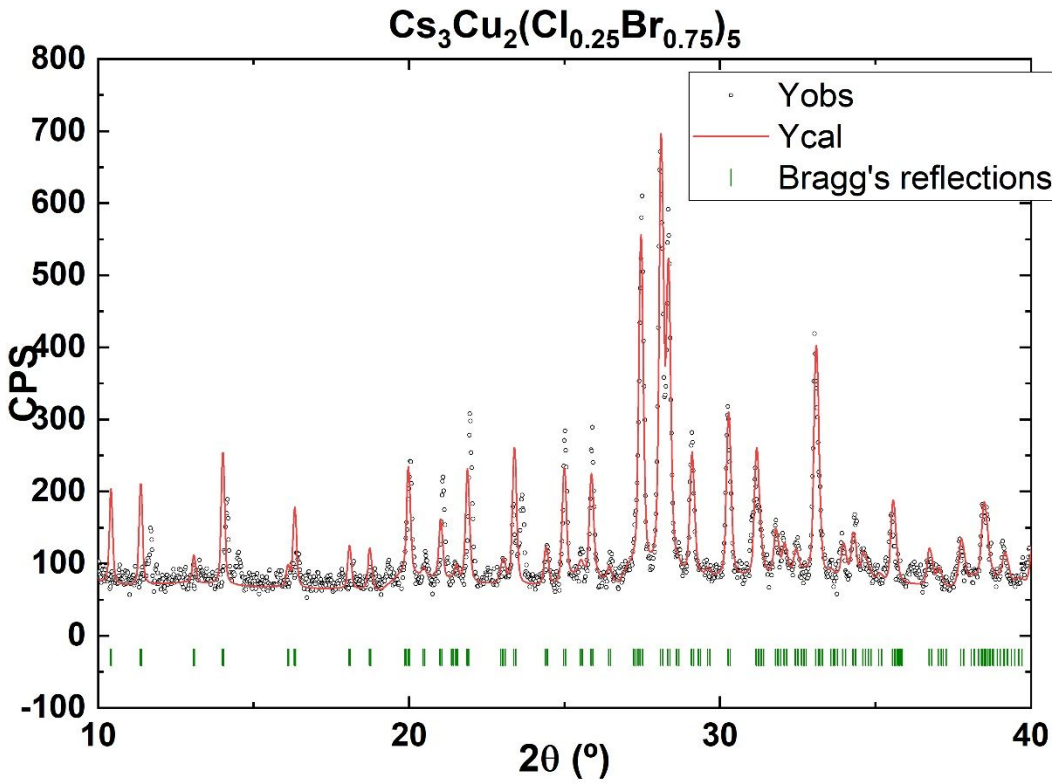

Figure S 20. Experimental (open circles) and fitted (red line) diffractograms. Caculated Bragg's reflections position in green. Compound given in title.

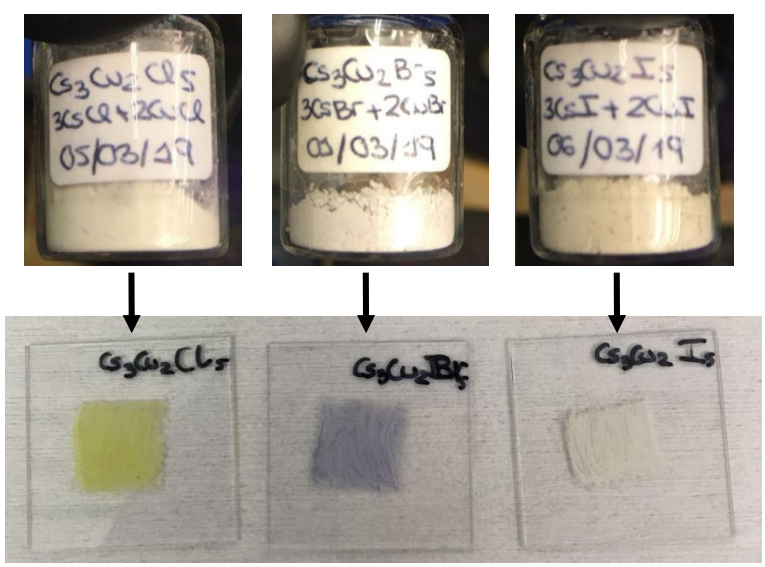

Figure S 21. Comparison of the colour of the powders for $Cs_3Cu_2X_5$ when they are kept inside a nitrogen filled glovebox (up) and when they are exposed to air and moisture for 24h (down).

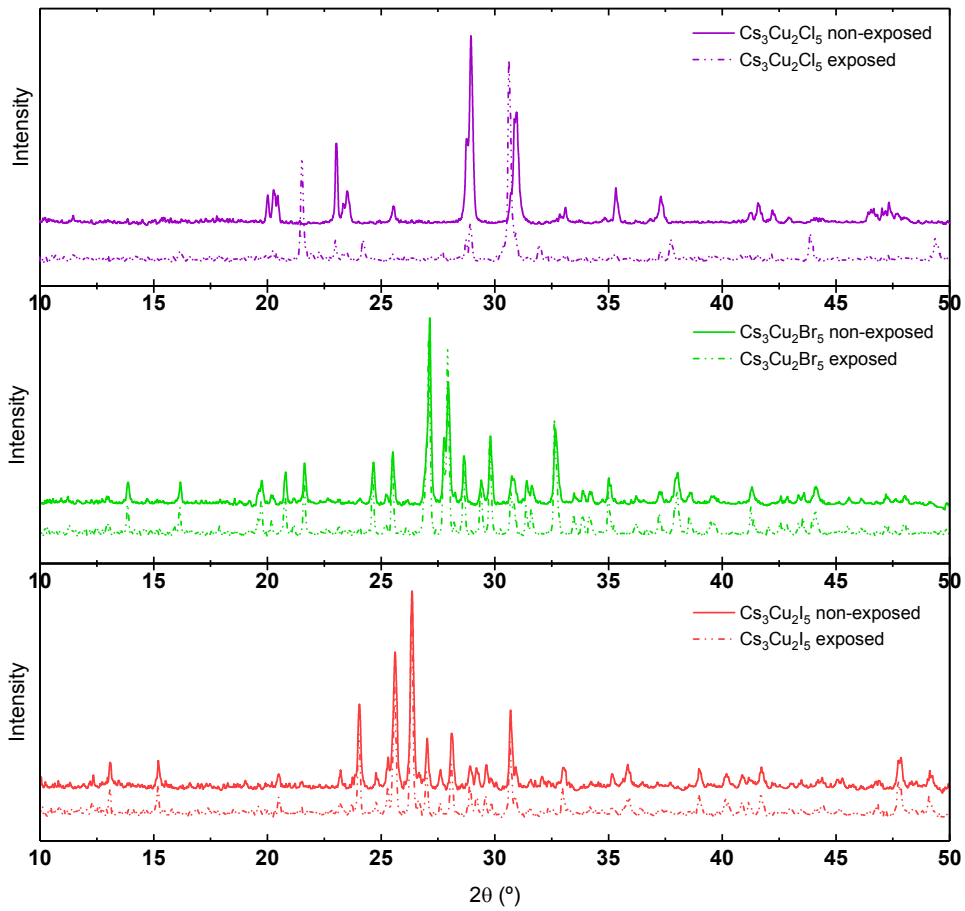

Figure S 22. XRD of the as-prepared powders from ball milling synthesis for pure-halide $Cs_3Cu_2X_5$ compounds. Non-exposed to air powders are presented with a straight line and the exposed ones, with a dashed line.

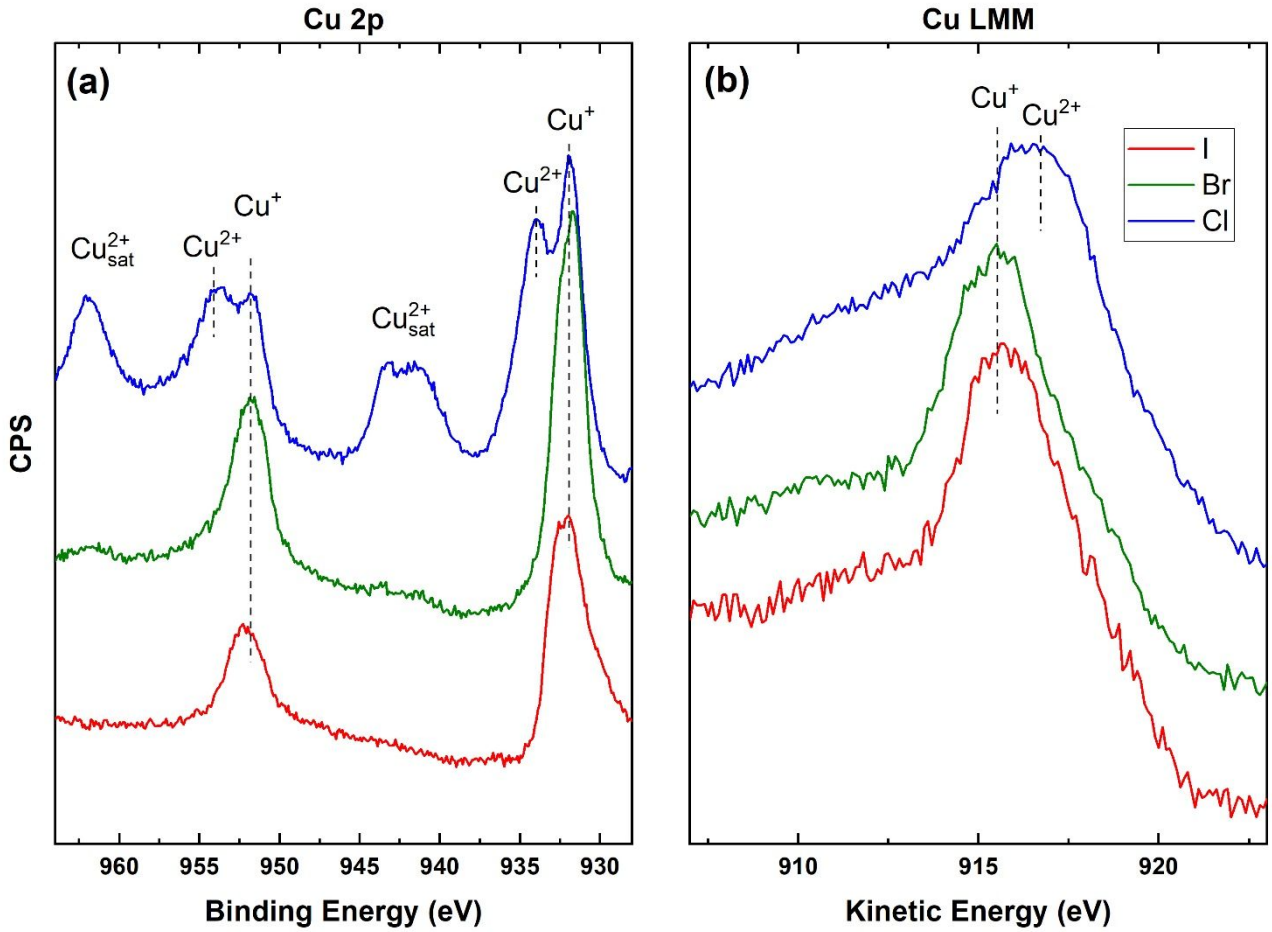

Figure S 23. XPS (a) and XAES (b) characterization of $Cs_3Cu_2X_5$ (X=Cl, Br, and I). Clear indications of Cu(II) exist in the Cs3Cu2Cl5 sample, demonstrating its lower stability in air.

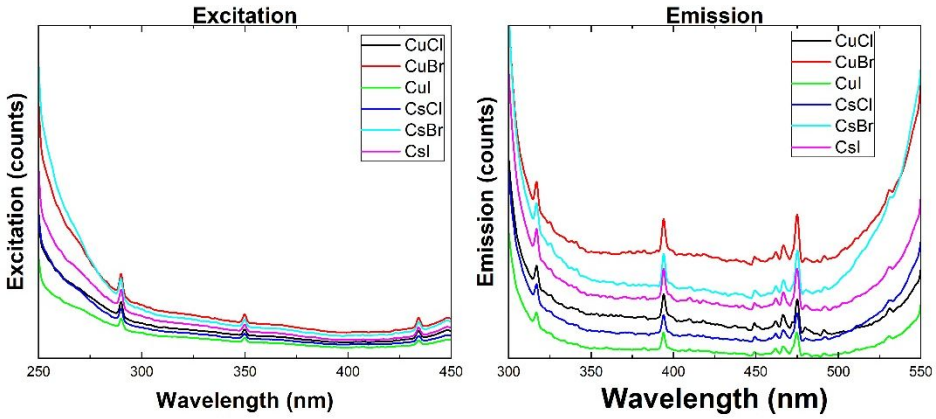

Figure S 24. Excitation and emission spectra of starting reagents. Excitation spectra are acquired for an emission at 475 nm, while emission spectra are acquired with an excitation set at 290 nm. No significant PL is observed from the different chemicals in these conditions. Low-intensity, sample-independent features are attributed to the instrument. The "tails" at the lower and higher wavelengths represented here are due to the excitation source itself (first and second harmonic).

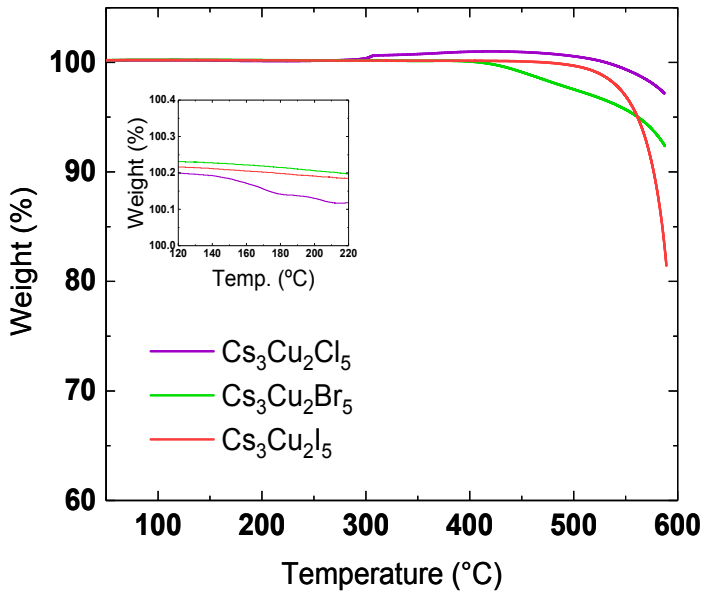

Figure S 25. Thermogravimetric analysis (TGA) of the pure-halide $Cs_3Cu_2X_5$ compounds when they are kept inside a nitrogen filled glovebox. A special zoom is presented in the zone of first weight loss for chloride compound, which could correspond with the formation of Cu_2O.

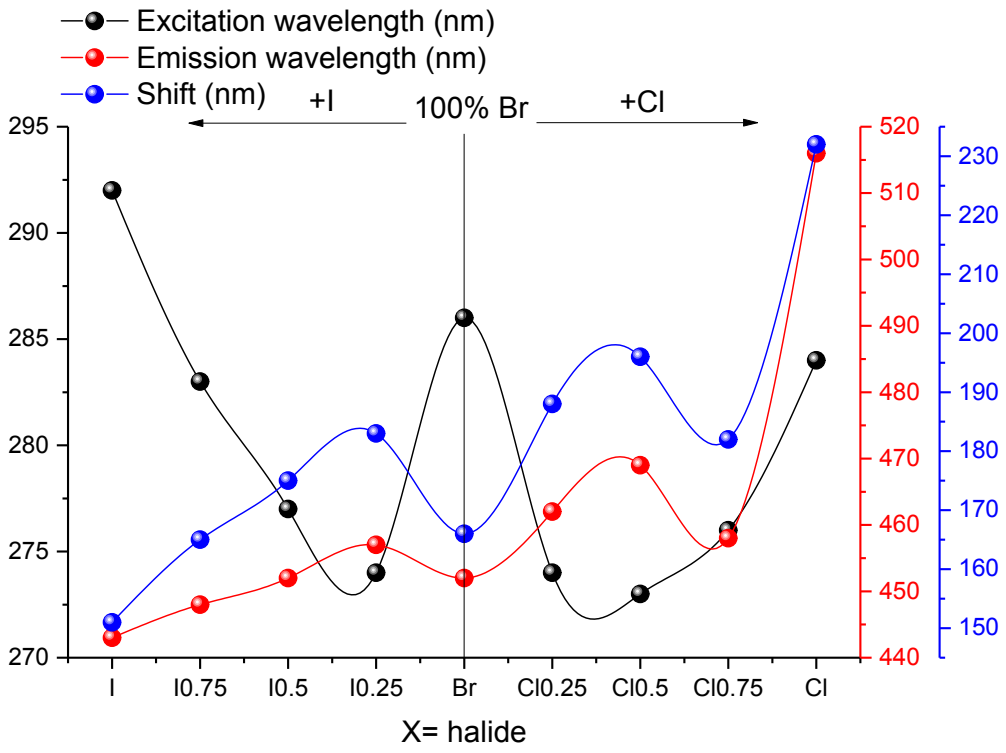

Figure S 26. Variation in the emission (red) and excitation (black) wavelength trend for all the species synthesized of $Cs_3Cu_2X_5$ structure (non-exposed powders). In blue in shown the difference between emission and excitation wavelengths.

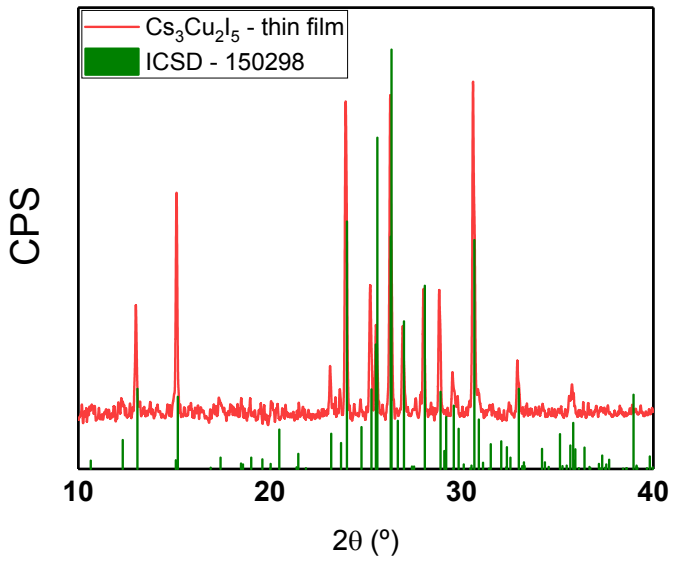

Figure S 27. XRD of the thin-films by solution processes of ball-milled powders of $Cs_3Cu_2I_5$ (red line) and its reference bulk pattern from the Inorganic Crystal Structure Database (ICSD) (green columns).

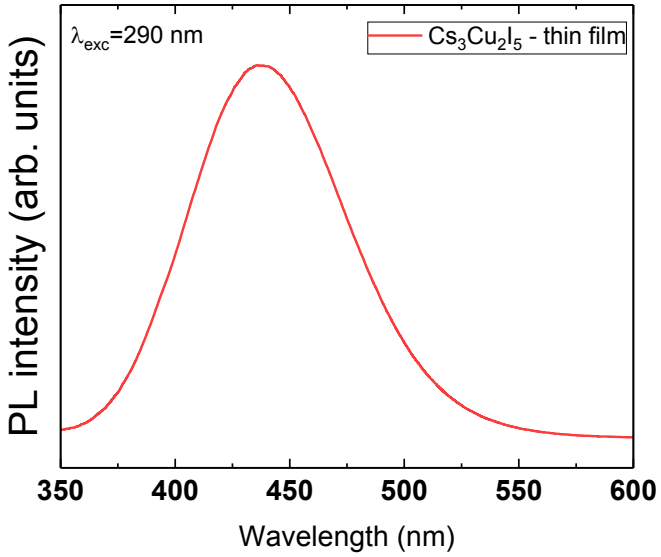

Figure S 28. Photoluminescence spectra of thin-films by solution processing of $Cs_3Cu_2I_5$.

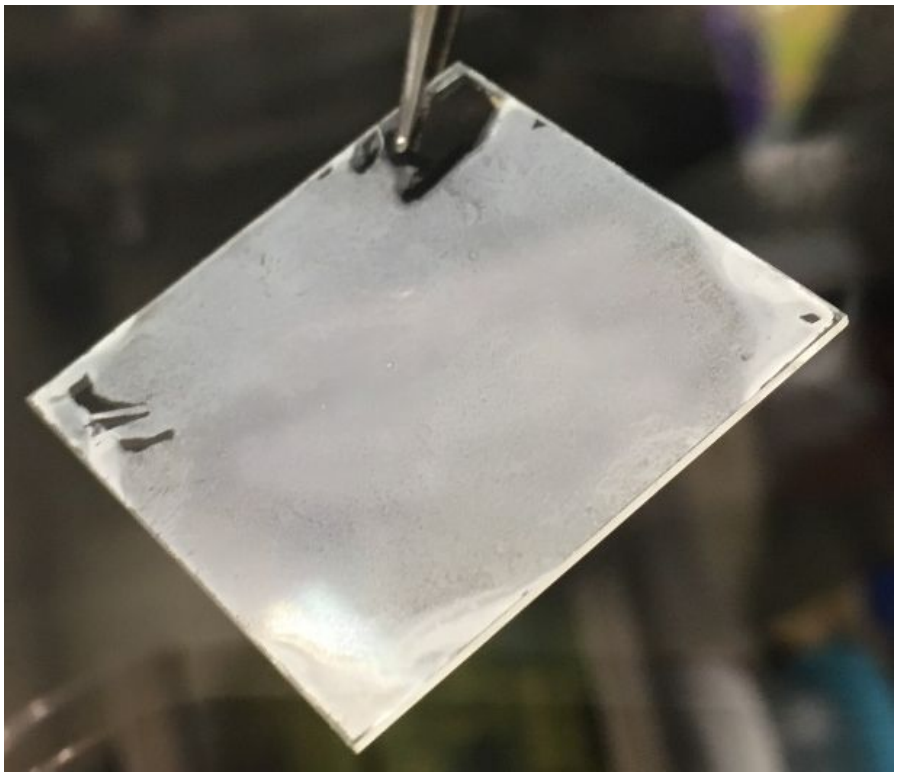

Figure S 29. Photograph of spin-coated $Cs_3Cu_2I_5$ film showing obvious inhomogeneities. Substrate is 3x3 cm.

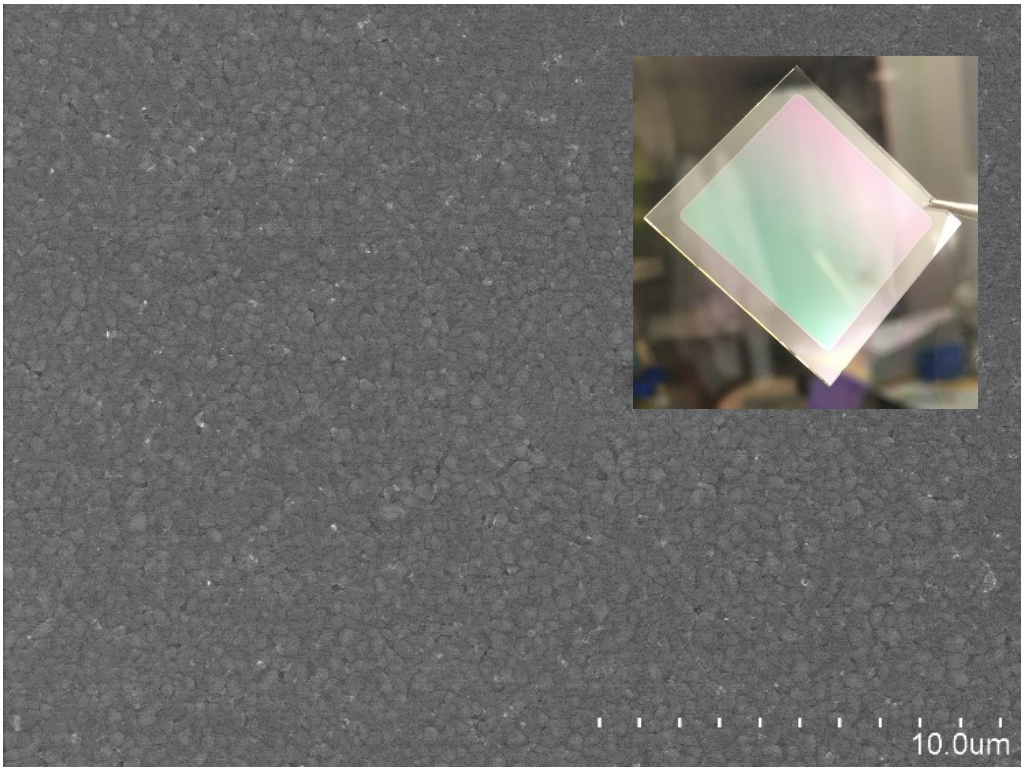

Figure S 30. SEM image and photograph (inset) of SSVD-film of $Cs_3Cu_2I_5$ showing good homogeneity.

SUPPLEMENTARY REFERENCES:

(1) Le Bail, A. Whole Powder Pattern Decomposition Methods and Applications: A Retrospection. *Powder Diffr.* **2005**, *20* (4), 316–326.

(2) Thompson, P., Cox, D.E., Hasting, J. B. Rietveld Refinement of Deybe-Scherrer Synchrotron X-Ray Data from Al2O3. *Jorunal Apply Crystallogr.* **1987**, *20*, 79–83.